Transmission and Reflection Analysis of Functional Coupled Cavity Components

Ulf Peschel, Andrew L. Reynolds, *Member, IEEE*, Belen Arredondo, Falk Lederer, Peter John Roberts, Thomas F. Krauss, and Peter J. I. de Maagt, *Senior Member, IEEE*

***Abstract*—This paper contributes to the ongoing discussion within the photonic crystal community by providing essential insight into the limiting conditions of the coupled cavity waveguiding mechanism. A theoretical and numerical description of coupled defects in PBG crystals is applied to quantify the conditions under which reflections occur within coupled cavity photonic crystal systems. We present an analysis of coupled cavity systems that form a straight and bent waveguide, a Y-shaped symmetric power splitter, and a waveguide incorporating two bends. The method is based on a weak interaction approach; the actual configuration of the defects (chain, lattice, bend, splitter, or anything else) enters the equations as a linear coupling between neighboring defects. The strength of this method is that many solutions of this system are known analytically, and that the band structure as well as the transmission and reflection response of the system can be determined.**

***Index Terms*—Electromagnetic crystals, periodic structures, photonic bandgap crystals.**

I. Introduction

PHOTONIC crystals (PCs) allow us to control the emission and propagation of electromagnetic waves to an extent that was previously not possible. These periodic structures have been investigated energetically in recent years. They are characterized by three parameters: the spatial period, the fractional volume of the constituent materials, and their dielectric constants. By properly selecting these parameters, one can generate gaps in the electromagnetic dispersion relation in which propagating electromagnetic modes are forbidden.

An ideal PC is constructed by the infinite repetition of identical structural units in space. Considerable effort in theoretical, experimental, and material fabrication research has predicted and demonstrated many of the properties of these ideal crystals. Introducing some disorder by placing a "defect unit" within an otherwise perfect photonic crystal can create localized transmission peaks within the forbidden bandgap of the structure. A single planar defect can form a mechanism for wave guiding.

Manuscript received August 31, 2001; revised April 9, 2002.

U. Peschel and F. Lederer are with the Friedrich-Schiller-Universität Jena, 07743 Jena, Germany.

A. L. Reynolds is with Nortel Networks, Harlow Laboratories, Harlow CM17 9NA, U.K.

B. Arredondo and P. J. I. de Maagt are with the Electromagnetics Division, European Space Research and Technology Centre, ESTEC, 2201 AG Noordwijk, The Netherlands.

P. J. Roberts is with the Defence Evaluation Research Agency, DERA Malvern, Malvern WR14 3PS, U.K.

T. F. Krauss is with the School of Physics and Astronomy, University of St. Andrews, St. Andrews Fife KY16 9SS, U.K.

Publisher Item Identifier S 0018-9197(02)05709-3.

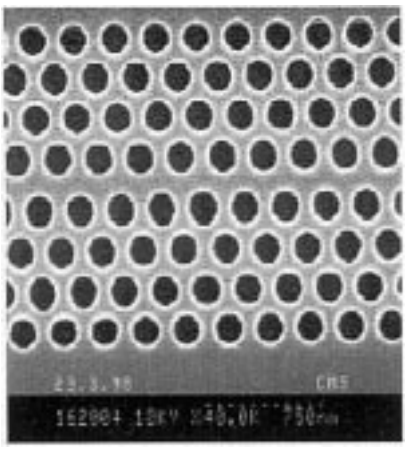

Fig. 1. Planar defect introduced into a hexagonal PC. Reproduced from [19] with permission.

Previous work [1] has suggested PC channel waveguides that consist of a line defect introduced into an otherwise perfect two-dimensional (2-D) crystal. Various bends, couplers, and add–drop multiplexers have also been proposed [2]–[4]. Some of the theoretical analysis was based on a single-mode air waveguide created within a square lattice of dielectric pillars. However, air waveguiding solutions in 2-D lack confinement in the third vertical direction. Furthermore, they require infinitely deep structures that can be readily analyzed but are more challenging to fabricate. A more pragmatic solution would be based on a dielectric waveguide and uses the inverse geometry, i.e., air holes in a dielectric host (see Fig. 1) [5], [6]. However, this complicates the issue because mode mixing occurs at interfaces and discontinuities such as bends. Conversely, dielectric channel guidance does have the added benefit that guiding is maintained within the periodic plane by total internal reflection, which is not the case for guides made from air. Dielectric guides are also inherently more compatible with conventional ridge waveguides and active elements, easing material mismatch and interface problems.

Another type of waveguide has attracted considerable attention recently. Instead of a continuous dielectric linear defect, this type makes use of a periodic chain of localized defects that have been either completely or partially in-filled. The introduction of several localized defects, within coupling distance of each other, opens up a mini-band of allowed transmission [7], [8]. Chains or cascades of localized defects form a mechanism for waveguiding, commonly referred to as coupled cavity waveguides (CCWs), a known concept in 1-D structures [9]. Experi-

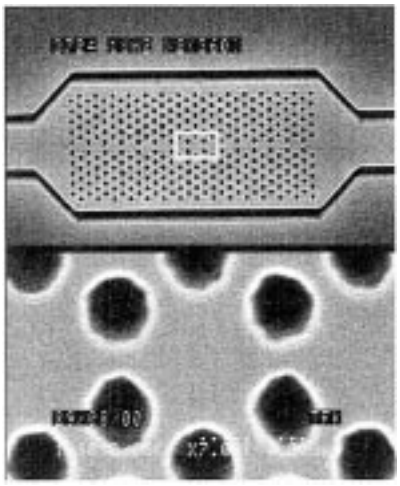

Fig. 2. A CCW into a hexagonal PC. The bottom picture shows the detail of an "in-filled" defect unit.

mental verification of 3-D CCWs has successfully been demonstrated for various PCs in the microwave regime by Bayindir, Temelkuran, and Ozbay [3], [10]–[12] and research into equivalent 2-D structures is underway at optical wavelengths [13], [14]. Fig. 2 shows a CCW and close up of the coupled cavity guiding region for optical wavelengths.

It has frequently been assumed that bends can be introduced into the waveguide path by taking advantage of the crystal's inherent lattice symmetry without consequential bend reflection loss. In this paper, we build upon our method based on a weak interaction approach, deriving explicit expressions for defect interaction [15], to demonstrate analytically that the mini passband created by CCW bends may only reach 100% transmission for a strict set of criteria. The basis is formed by a system of coupled ordinary differential equations for the field amplitudes for individual defects. The actual configuration of the defects (chain, lattice, bend, splitter, or anything else) enters the equations as a linear coupling between neighboring defects. The strength of this method is that many solutions of this system are known analytically; the band structure as well as the transmission and reflection response of the system can be determined. In this paper, this approach is applied to elegantly describe CCW waveguides, bends, and power splitters, which are difficult to simulate with transfer matrix codes. The analysis intuitively determines the reflection and transmission properties of the structure providing essential insight into the limiting conditions of the CCW mechanism.

II. Coupled-Mode Theory for Coupled Defect Systems

The method is described in full detail elsewhere [15]; therefore, only the main principle is reiterated here. Coupled-mode theory provides us with a deeper insight into the energy transfer dynamics of coupled defect systems. In the case of weak interaction, the modal field structure of individual defects remains unchanged, and only the respective field amplitudes evolve in time. Provided that the individual defects are similar and single mode, the dynamics of the coupled defect system are described by a set of ordinary differential equations, generally

$$i\,\frac{d}{dt}\,a_i = (\omega_0 - i\gamma_0 - i\gamma_i)a_i - \sum_{\substack{j=1\\ j\neq i}}^{N} c_{ij}a_j + \hat{\tau}_i a_{\mathbf{in}_i} \qquad (1)$$

where the sum accounts for the energy transfer between the N defect modes, ω_0 is the eigenfrequency of the defect, and $\gamma_0 + \gamma_i$ is the decay rate. There are two possible reasons for this decay. First, dielectric losses as well as out-of-plane-scattering into substrate or cladding give rise to energy losses. The magnitude of these losses should not depend on the position of the defect within the crystal and is represented by γ_0. Second, further decay is attributed to power transfer to the environment of the crystal and is represented by γ_i. Real PC systems are finite; therefore, boundaries play an important role. The fields attached to the defect transform from bound states, which decay exponentially into every space direction to leaky modes, which have oscillating tails outside the PC and contribute to either the transmitted or the reflected fields. The same defect mode can be excited by external radiation allowing for an interaction of the coupled defect system with its environment. Obviously, γ_i is different from zero for defects close to the side facet or interface of the crystal. The driving field at the defect $a_{\mathbf{in}_i}$ couples to the outermost defects via $\hat{\tau}_i$ and is represented in the evolution integral via the term $\hat{\tau}_i a_{\mathbf{in}_i}$. As with γ_i, this term will play a role only at the outermost defects.

Conservation of energy determines the relations between the coupling to external fields and radiative losses (see [15]). The transmitted field is always proportional to the amplitudes of the defect amplitudes closest to the output facet. The overall dynamical response of the defect system is determined by the coupling coefficients c_{ij}. They are real valued and given by the mutual overlap between the field structures of the defect modes $\vec{E}_i$ and $\vec{E}_j$ and the changes of the dielectric constant $\delta\varepsilon_{\mathrm{R}}$, which has induced the defects

$$c_{ij} = \omega_0 \frac{\int d^3r \delta\varepsilon_{\mathrm{R}} \vec{E}_i \vec{E}_j}{\int d^3r \varepsilon_{\mathrm{R}} \left|\vec{E}_i\right|^2}. \qquad (2)$$

III. Coupled-Mode Theory for Photonic Components

As demonstrated in [15], coupled-mode theory can provide us with insight into the frequency response and transmission characteristics of defect lattices. Previously it was applied to a superlattice of defects, but the main potential of this approach is that it can be applied to create an elegant description of CCW components such as waveguides, bends, and power splitters [16], which are difficult to simulate with transfer matrix codes. Here we sketch the procedure while evaluating the dynamical response of a defect chain.

A. Straight Defect Chain

A simple CCW chain consists of regularly spaced defects (see Fig. 2). For the case of a straight chain, the next-nearest

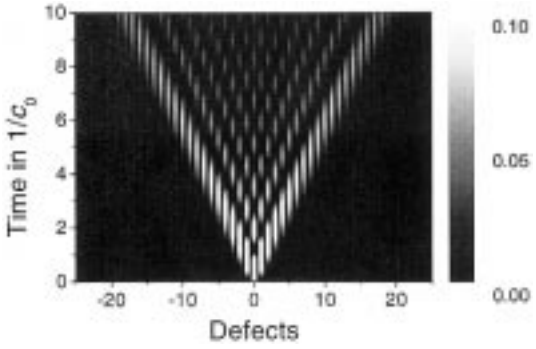

Fig. 3. Field evolution on a chain of coupled defects after an excitation of defect 0 at time 0 (the power at the individual defects is plotted).

neighbor interaction has to cover double the spacing compared with nearest neighbor interaction. Because all the interactions should be weak and the fields of defect modes decay exponentially in space, only the nearest neighbor interaction is considered. Hence, the amplitudes of the defect modes far from interfaces follow the evolution equation

$$i\frac{d}{dt}a_n = (\omega_0 + i\gamma_0)a_n - c_0(a_{n-1} + a_{n+1}). \tag{3}$$

For vanishing losses ($\gamma_0 = 0$), there are waves traveling along the chain as

$$a_n(t) = a_{\pm}\exp(-i\omega t \pm i\alpha n). \tag{4}$$

The wavenumber α and the frequency ω are linked to each other via the dispersion relation

$$\omega = \omega_0 - 2c_0\cos(\alpha) \tag{5}$$

which also defines the mini band structure of the CCW. To get an impression of the dynamical response of the straight defect chain, we assume a point-like excitation of a single element of the CCW. This could be either by spontaneous emission or by some external excitation. We define our initial condition as

$$a_n(t=0) = 0 \quad \text{for } n \neq 0 \quad \text{and} \quad a_0(t=0) = a.$$

The solution of (3) is known [15] as

$$a_n(t) = a(-i)^n\exp(-i\omega_0 t - \gamma_0 t)\mathrm{J}_n(2c_0 t) \tag{6}$$

where J_n is the Bessel function of order n. The respective spatial temporal field evolution for vanishing losses is displayed in Fig. 3. Obviously the excitation rapidly expands in space. The respective front is determined by those frequency components of the mini-band with the maximum group velocity

$$v_g = \frac{\partial\omega}{\partial\alpha} \tag{7}$$

which amounts to $\pm 2c_0$ for $\alpha = \pm\pi/2$ or $\omega = \omega_0$. Pulses with a frequency in the middle of the mini-band travel with the highest velocity. This maximum velocity limits the speed of any signal transfer along the chain.

B. Transmission Response of a Bend

Next we discuss the spectral response of a slightly more involved photonic component—a bend in a defect guide in a hexagonal PC lattice. For a bending angle of 120° within a hexagonal lattice, defects close to the corner may start to interact via next-nearest neighbor interaction [coupling coefficient c_1, see Fig. 4(a)]. To demonstrate the effect of nonvanishing next-nearest-neighbor interaction, we assume additional losses to be negligible ($\gamma_0 = 0$). The respective evolution equations are

$$n < -1, \quad n = 0 \quad \text{or} \quad n > 1:$$

$$i\frac{d}{dt}a_n = \omega_0 a_n - c_0(a_{n-1} + a_{n+1}) \tag{8a}$$

$$n = \pm 1:$$

$$i\frac{d}{dt}a_{\pm 1} = \omega_0 a_{\pm 1} - c_0(a_0 + a_{\pm 2}) - c_1 a_{\mp 1}. \tag{8b}$$

For a monochromatic excitation, the field before the bend ($n \leq -1$) consists of incident and reflected components

$$a_n = a_{\mathbf{in}}\exp[i\alpha(n+1) - i\omega t] + a_\rho\exp[-i\alpha(n+1) - i\omega t] \tag{9a}$$

where only the transmitted fields leave the bend toward defects, with corresponding increasing n as follows:

$$a_n = a_\tau\exp(i\alpha n - i\omega t). \tag{9b}$$

All the waves are eigensolutions of the straight defect chain and obey the dispersion relation (5). Note that the dispersion relation (5) means that the defect chain itself is only transparent in a limited frequency domain $(\omega - \omega_0)^2 < 4c_0^2$. Otherwise α is imaginary and waves are evanescent. Inserting (9a) and (9b) into (8), we can determine the reflectivity of the bend analytically as shown in (10), at the bottom of the page, where $\delta\omega = \omega - \omega_0$ is the detuning from the defect frequency. Hence, the reflection of the bend can only vanish if next-nearest neighbor interaction is negligible ($c_1 = 0$). In this case, the evolution equations of the bend (8) become similar to those of the straight defect chain (3), and the system remains transparent. For strong next-nearest neighbor interaction, the bend is transparent at a particular frequency point $\delta\omega = 2c_0^2/c_1$, which is only in the transparency region of the defect chain for $c_1 > c_0$. Fig. 4(b) shows plots of the reflection response of a bend for some particular values of c_1/c_0. For realistic values of c_1 (in [15] c_1/c_0 was determined to amount to about 1/3 in case of a 1 in 3 defect lattice) the reflection is noticeable and pronounced at the band edges.

$$\rho = \frac{a_\rho}{a_{\mathbf{in}}} = \frac{\delta\omega c_1\left[2c_0^2 - \delta\omega c_1\right]}{\delta\omega^4 + 2\delta\omega c_0^2 c_1 - (c_1^2 + 3c_0^2)\,\delta\omega^2 + [c_0^2 - \delta\omega^2/2]\left[\delta\omega^2 + i\delta\omega\sqrt{4c_0^2 - \delta\omega^2}\right]} \tag{10}$$

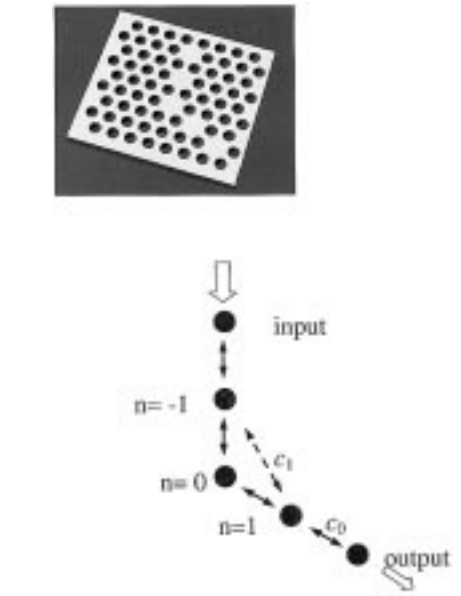

(a)

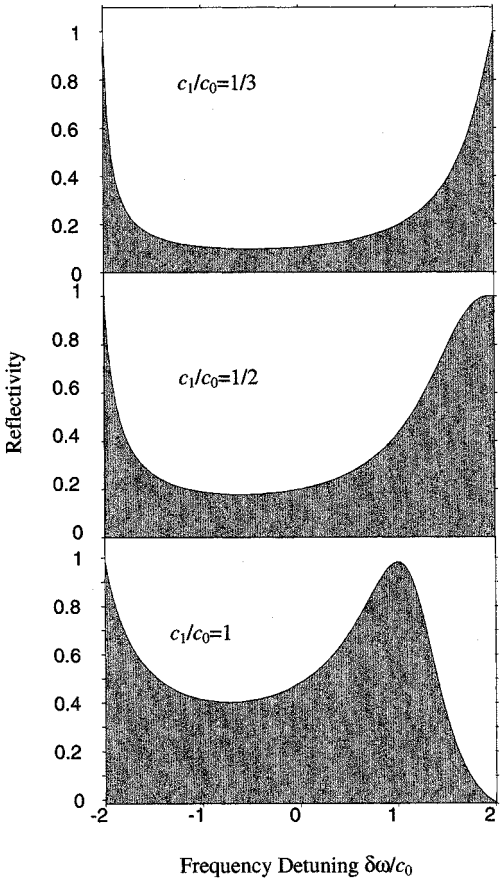

(b)

Fig. 4. Spectral response of a bend in a defect chain in a hexagonal PC lattice. (a) Top: image of a bend in a 1-in-2 defect chain. Middle: schematic drawing. (b) Reflection for varying ratio of the next-nearest to nearest neighbor interaction.

However, for a hexagonal lattice and a bending angle of 60°, the defects $n = \pm 1$ interact via the next-nearest neighbor interaction and therefore $c_1/c_0 = 1$ resulting in significant levels of reflection. It is interesting to note that next-nearest neighbor interaction not only reduces the transmission of a bend, but can also introduce new peaks into an overall transmission response. For $c_1 \neq 0$, the bend gives rise to the formation of a bound state. The frequency and mode profile of the bound state can be determined by setting $a_{\text{in}} = 0$ in (9a) and solving with an imaginary value of α. A bound state with even symmetry ($a_1 = a_{-1}$) always exists. However, the eigenfrequency is outside the transparent region of the defect chain and is determined by

$$\omega = \omega_0 - 2\text{sgn}(c_1)|c_0|\cosh(\kappa) \tag{11a}$$

where κ is a solution of the equation

$$\exp(2\kappa) - \left|\frac{c_1}{c_0}\right| [\exp(\kappa) + \exp(-\kappa)] = 1.$$

For a strong next-nearest neighbor interaction ($c_1 > c_0$), a second bound state with odd symmetry ($a_1 = -a_{-1}$, $a_0 = 0$) appears on the other side of the transparent domain with an eigenfrequency

$$\omega = c_1 + \frac{c_0^2}{c_1} + \omega_0. \tag{11b}$$

A complete device will show a transmission peak outside the mini-band, if the frequency of the incident wave hits one of the eigenfrequencies given in (11a) and (11b).

C. Response of a Splitter

A simple power splitter is shown schematically in Fig. 5(a). To simplify the analytical treatment, we restrict the analysis to nearest neighbor interactions and assume vanishing losses. The power splitter is assumed to be symmetric, but the coupling coefficients in the input and output channels can be different. The respective evolution equations are

$$n<0$$
$$i\frac{d}{dt}a_n = -c_{\text{input}}(a_{n-1} + a_{n+1}) + \omega_0 a_n \tag{12a}$$
$$n=0$$
$$i\frac{d}{dt}a_0 = -c_{\text{input}}a_{-1} - c_{\text{output}}\left(a_1^{\text{r}} + a_1^{\text{l}}\right) + \omega_0 a_0 \tag{12b}$$
$$n>0$$
$$i\frac{d}{dt}a_n^{\text{r/l}} = -c_{\text{output}}\left(a_{n-1}^{\text{r/l}} + a_{n+1}^{\text{r/l}}\right) + \omega_0 a_n^{\text{r/l}}. \tag{12c}$$

For a monochromatic excitation, the field before the splitter consists of incident and reflected components

$$a_n = a_{\text{in}}\exp(i\alpha_{\text{input}}n - i\omega t) + a_\rho \exp(-i\alpha_{\text{input}}n - i\omega t) \tag{13a}$$

and only the transmitted fields leave the splitter toward defects with positive n

$$a_n^{\text{r/l}} = a_\tau^{\text{r/l}}\exp\left(i\alpha_{\text{output}}n - i\omega t\right). \tag{13b}$$

The respective propagation constants are elements of the band structure of the defect chains and are determined by the actual frequency detuning $\delta\omega = \omega - \omega_0$ as

$$\delta\omega = -2c_{\text{input/output}}\cos\alpha_{\text{input/output}}. \tag{13c}$$

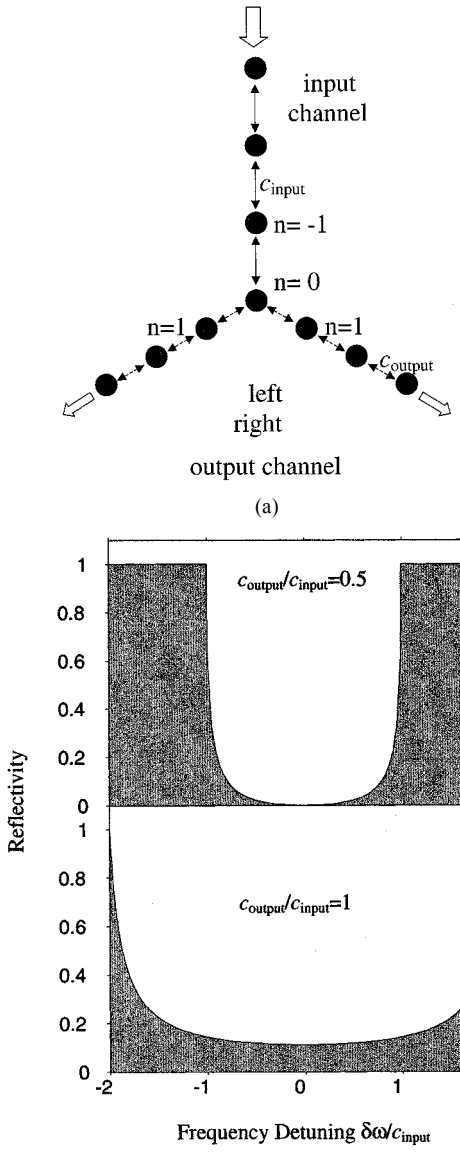

Fig. 5. Spectral response of a Y-junction. (a) Schematic drawing. (b) Reflection for different ratios of the coupling constants.

The spectral response of the splitter is investigated for frequencies, where the input channel is transparent. By assuming that the coupling coefficient in the output channels is similar, symmetry dictates that the transmitted fields are equal in the right and left output channels. Inserting (13a)–(13c) into (12), we can determine the reflectivity of the junction analytically as shown in (14) at the bottom of the page.

Equation (14) can only vanish if the real and imaginary parts of its numerator cross zero simultaneously. This happens for particular points in parameter space only, namely for $c_{\mathrm{input}}/2 = c_{\mathrm{output}}$ and $\delta\omega = 0$. Generally the splitter reflects some of the power [see Fig. 5(b)]. Equation (14) can be simplified for the case of equal coupling in input and output channels ($c_{\mathrm{input}} = c_{\mathrm{output}} = c_0$). In this case, the portion of the reflected energy amounts to

$$|\rho|^2 = \frac{1}{9 - 2(\delta\omega/c_0)^2}. \tag{15}$$

Note that, as in the case of the simple bend, the slow waves at the edges of the mini-band experience the strongest reflection. The transparent spectral range is effectively narrowed by the action of the splitter. This result does not change, even if long-range coupling is taken into account.

IV. Photonic Components in Real Crystals

Having evaluated the response of different photonic components, we evaluate how these structures behave in real crystals by examining in more detail the influence of losses and boundaries.

A. Transmission of a Straight Defect Chain

The straight defect chain is homogenous; therefore, reflection only occurs at external boundaries. Assume the chain to be extended between two interfaces, the first ($n = 1$) and the last defects ($n = N$) will experience additional loss ($\gamma_1 > 0$, $\gamma_N > 0$) and lack one neighbor. While (3) is still valid within the chain, the defects at both ends are now described by a slightly different evolution equations

$$i\frac{d}{dt}a_1 = (\omega_0 - i\gamma_0 - i\gamma_1)a_1 - c_0 a_2 + \hat{\tau}a_{\mathrm{in}} \tag{16a}$$

$$i\frac{d}{dt}a_N = (\omega_0 - i\gamma_0 - i\gamma_N)a_N - c_0 a_{N-1}. \tag{16b}$$

Here we assume defect $n = 1$ to be driven by the external radiation a_{in}. The overall transmitted field a_τ is proportional to the field amplitude at defect N like $a_\tau = c_\tau a_N$. Radiative damping, represented by γ_N, and coupling to external radiation are related to each other due to energy conservation $|c_\tau|^2 = 2\gamma_N$. The first defect of the chain also radiates to outer space, interfering with the field that is directly reflected by the crystal interface. Consequently, the overall reflectivity depends not only on the CCW itself, but also on the shape of the excitation and on the structure of the surface of the crystal.

We concentrate here on the transmission of the structure. Because the efficiency of the excitation represented by $\hat{\tau}$ is not known, we can only give qualitative estimates of the transmission. Even in the presence of losses, forward and backward propagating waves exist, and each defect amplitude is a superposition of two wave amplitudes

$$a_n(t) = a_+ \exp(-i\omega t + i\alpha n) + a_- \exp(-i\omega t - i\alpha n) \tag{17a}$$

$$\rho = \frac{a_\rho}{a_{\mathrm{in}}} = -\frac{\exp(i\alpha_{\mathrm{output}}) - \exp(-i\alpha_{\mathrm{output}}) + c_{\mathrm{input}}/c_{\mathrm{output}}\exp(-i\alpha_{\mathrm{input}})}{\exp(i\alpha_{\mathrm{output}}) - \exp(-i\alpha_{\mathrm{output}}) + c_{\mathrm{input}}/c_{\mathrm{output}}\exp(i\alpha_{\mathrm{input}})} \tag{14}$$

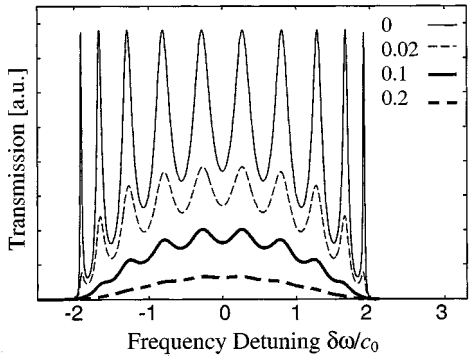

Fig. 6. Transmission of a straight CCW for varying losses γ_0/c_0 (number of defects: 10, strength of radiative losses at the interfaces: $\gamma_1 = \gamma_N = 0.4c_0$).

where the complex wavenumber α and the frequency detuning are now linked by

$$\delta\omega + i\gamma_0 = -2c_0\cos(\alpha). \tag{17b}$$

Inserting (17a) and (17b) into (16) and solving the respective system of linear equations determines the transmission as shown in (18) at the bottom of the page.

Fig. 6 shows a typical transmission spectrum of a straight defect chain for varying losses γ_0. As expected, every single defect produces a separate peak in the transmission band. In the middle of the mini-band, the peaks are wider, because the excited wave travels fast and decays quickly [see (5) and (7)]. Increasing losses reduce the overall transmission and wash out the internal structure of the response function.

B. Transmission of a CCW With Two Internal Bends

Finally, we evaluate the spectral response of a more complicated structure—a CCW with two internal bends [see Fig. 7(a)]. Such structures were used to evaluate the efficiency of waveguide bends in PCs [18]. Here we demonstrate that a nonzero next-nearest neighbor interaction can alter the performance of such a device considerably. Basically, the transmission function of this structure can also be determined analytically in the same manner as was done above for the straight CCW. However, because a system of six coupled linear equations has to be solved (every bend adds two equations), the resulting analytical solution is too bulky to be reproduced.

If only neighboring defects interact, the spectral response is that of a straight chain of defects. As soon as the next-nearest neighbor interaction comes into play, the whole transmission function becomes distorted [see Fig. 7(b)]. Induced changes are asymmetric in frequency space and can clearly be distinguished from any changes, which are induced by losses; compare Figs. 6 and 7(b). It is interesting to note that peaks are shifted outside the mini-band. For a frequency detuning of $\delta\omega < -2c_0$, the CCW is

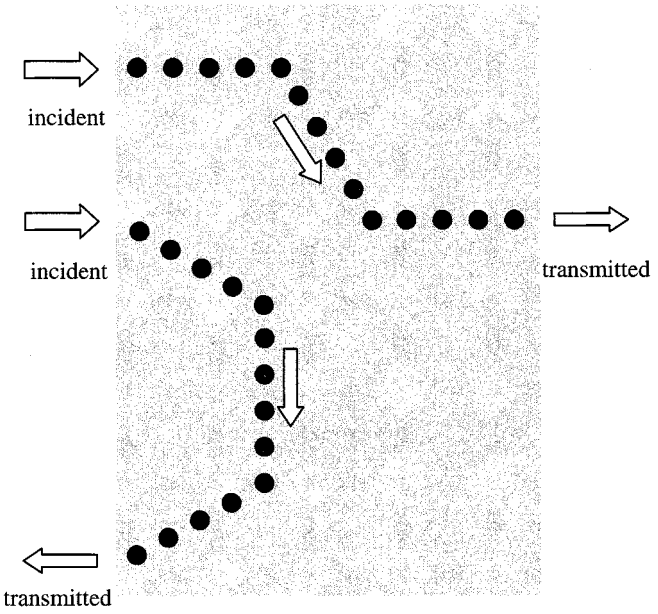

(a)

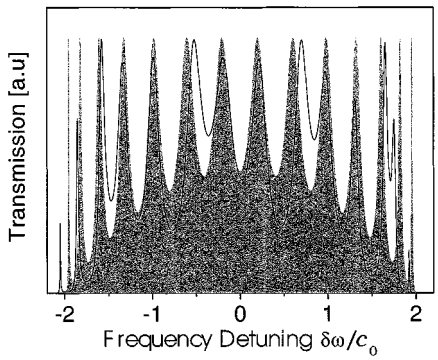

(b)

Fig. 7. Transmission of a double-bend structure: (a) two possible realizations and (b) spectral response (gray area: without next-nearest neighbor interaction $c_1 = 0$, solid line: next-nearest neighbor interaction in the bends $c_1 = c_0/3$, $\gamma_1 = \gamma_N = 0.4c_0$).

not transparent and the resonance originates from bound states formed in the bends [see (11a)].

V. Conclusion

We have shown that a set of coupled ordinary differential equations describing defect coupling within a photonic crystal creates a powerful analytical tool. This tool has then been applied to analyze a straight, coupled cavity waveguide, a waveguide bend, and a symmetrical power splitter. Next-nearest neighbor interactions between defects have shown to be critical in governing the reflection from a waveguide bend. The overall reflectivity of the crystal will also depend on the shape and type of interface at the surface of the crystal. We have shown

$$\tau(\delta\omega) = \frac{\hat{\tau}c_\tau/c_0\sin\alpha}{\frac{\gamma_1\gamma_N}{c_0^2}\sin[\alpha(N-1)] + i\left(\frac{\gamma_1}{c_0}+\frac{\gamma_N}{c_0}\right)\sin(\alpha N) - \sin[\alpha(N+1)]} \tag{18}$$

that, generally, power will always be reflected from a CCW splitter as the criteria for zero reflection are quite stringent. Furthermore, a CCW splitter narrows the spectral range of the CCW system.

REFERENCES

[1] J. D. Joannopoulos, R. D. Meade, and J. N. Winn, *Photonic Crystals Molding the Flow of Light*. Princeton, NJ: Princeton Univ. Press, ISBN 0-691-03 744-2.

[2] A. Mekis, J. C. Chen, I. Kurland, S. Fan, P. R. Villeneuve, and J. D. Joannopoulos, "High transmission through sharp bends in photonic crystal waveguides," *Phys. Rev. Lett.*, vol. 77, p. 3787, 1996.

[3] B. Temelkuran and E. Ozbay, "Experimental demonstration of photonic crystal based waveguides," *Appl. Phys. Lett.*, vol. 74, no. 4, pp. 486–488, 1999.

[4] G. Tayeb and D. Maystre, "Rigorous theoretical study of finite-size two-dimensional photonic crystals doped by microcavities," *J. Opt. Soc. Amer. A*, vol. 14, p. 3323, 1997.

[5] A. R. McGurn, "Photonic crystal circuits: Localized modes and waveguide couplers," *Phys. Rev. B*, vol. 65, p. 075 406, 2002.

[6] ——, "Photonic crystal circuits," *Physica B*, vol. 296, pp. 201–209, 2001.

[7] N. Stefanou and A. Modinos, "Impurity bands in photonic insulators," *Phys. Rev. B*, vol. 57, p. 12 127, 1998.

[8] A. Yariv, Y. Xu, R. K. Lee, and A. Scherer, "Coupled-resonator optical waveguide: A proposal and analysis," *Opt. Lett.*, vol. 24, no. 11, pp. 711–713, 1999.

[9] H. Haus and Y. Lai, "Theory of cascaded quarter wave shifted distributed feedback resonators," *IEEE J. Quantum Electron.*, vol. 28, pp. 205–213, Jan. 1992.

[10] M. Bayindir, B. Temelkuran, and E. Ozbay, "Tight-binding description of the coupled defect modes in three-dimensional photonic crystals," *Phys. Rev. Lett.*, vol. 84, no. 10, pp. 2140–2143, 2000.

[11] ——, "Propagation of photons by hopping: A waveguiding mechanism through localized coupled-cavities in three-dimensional photonic crystals," *Phys. Rev. B*, vol. 61, p. R11855, 2000.

[12] M. Bayindir and E. Ozbay, "Heavy photons at coupled-cavity waveguide band edges in a three-dimensional photonic crystal," *Phys. Rev. B*, vol. 62, no. 4, pp. R2247–R2250, 2000.

[13] T. J. Karle, D. H. Brown, R. Wilson, M. Steer, and T. F. Krauss, "Planar photonic crystal coupled cavity waveguides," IEEE J. Select. Topics Quantum Electron., to be published.

[14] S. Olivier, C. Smith, and M. Rattier, "Miniband transmission in a photonic crystal coupled-resonator optical waveguide," *Opt. Lett.*, vol. 26, no. 13, pp. 1019–1021, 2001.

[15] A. L. Reynolds, U. Peschel, F. Lederer, P. J. Roberts, T. F. Krauss, and P. J. I. de Maagt, "Coupled defects in photonic crystals," *IEEE Trans. Microwave Theory Tech.*, vol. 49, pp. 1860–1867, Oct. 2001.

[16] M. Bayinidir, B. Temelkuran, and E. Ozbay, "Photonic crystal based beam splitters," *Appl. Phys. Lett.*, vol. 77, no. 24, pp. 3902–3904, 2000.

[17] A. Yariv, *Optical Electronics*, 4th ed. Philadelphia, PA: Saunders College Publishing, 1991, pp. 519–524.

[18] E. Chow, S. Y. Lin, J. R. Wendt, S. G. Johnson, and J. D. Joannopoulos, "Quantitative analysis of bending efficiency in photonic-crystal waveguide bends at $\lambda = 1.55$ μm wavelengths," *Opt. Lett.*, vol. 26, no. 5, pp. 286–288, 2001.

[19] C. J. M. Smith, R. M. De La Rue, H. Benisty, U. Oesterle, T. F. Krauss, D. Labilloy, C. Weisbuch, and R. Houdre, "In plane microcavity resonators with two-dimensional photonic bandgap mirrors," *Proc. IEE—Optoelectron.*, vol. 145, no. 6, pp. 373–378, Dec. 1998.

Ulf Peschel was born in Jena, Germany, in 1964. He received the diploma and the Ph.D. degree in physics from the Friedrich-Schiller-Universität Jena, Jena, Germany, in 1990 and 1994, respectively.

Since then, he has been with the Friedrich Schiller Universität Jena. Between 1998 and 1999, he spent one year at the University of Glasgow, U.K. His research interests include micro optics, nonlinear optics, and nonlinear dynamics.

Andrew L. Reynolds (M'xx) was born in Birmingham, U.K., in 1974. He received the M.Eng. and Ph.D. degrees in 1996 and 2000, respectively from the University of Glasgow, Glasgow, U.K.

In 1997, he spent one year as a Young Graduate Trainee in the Antenna Section of the European Space Research and Technology Centre (ESTEC), Noordwijk, The Netherlands. His research interests are focused on photonic bandgap materials to antenna and optoelectronic applications.

Belen Arredondo was born in Madrid, Spain, in 1975. She received the Diploma in physics (with Honors) from the University of Kent, Canterbury, U.K., and the M.S. degree in physics from the Universidad Complutense, Madrid, Spain, in 1997 and 1999, respectively.

She worked for several months at Price Water House Coopers. In June 2000, she joined the Antenna Section of the European Space Research and Technology Centre (ESTEC), Noordwijk, The Netherlands, as a Research Fellow. Her research is focused on waveguiding using periodic structures in the microwave regime.

Falk Lederer was born in Tannenbergstual, Germany, in 1948. He received the Diploma degree and Ph.D. degree in physics from Friedrich-Schiller Universität Jena, Jena, Germany, in 1972 and 1977, respectively.

He is currently the Head of the Photonics Group, Friedrich-Schiller Universität Jena. His research interests include nonlinear optics, integrated optics, and optical communications.

Peter John Roberts was born in Dover, U.K., in 1968. He received the B.A. degree in physics and the Ph.D. degree in theoretical condensed matter physics from Oxford University, Oxford, U.K., in 1989 and 1992, respectively.

Since then, he has worked at the Defence Evaluation and Research Agency (DERA), Malvern, U.K. His research interests include photonic bandgap materials, waveguide, optics, nanowires, statistical optics, and signal processing.

Thomas F. Krauss was born in 1964 in Rheinbach, Germany. He received the Dipl.-Ing. degree in photographic engineering from FH Koeln, Germany, in 1989 and the Ph.D. degree in electrical engineering from the University of Glasgow, Glasgow, U.K., in 1992.

In 1993, he won an EPSRC Research Fellowship in the area of photonic bandgaps, thereby initiating a new field at Glasgow University, followed by a Royal Society Research Fellowship in 1995. He is one of the pioneers of waveguide-based, high index contrast photonic microstructures in semiconductors, and made the first demonstration of 2-D photonic bandgap effects at optical wavelengths (1996). He spent a year at the California Institute of Technology, Pasadena, and the University of California at Los Angeles in 1997, working on photonic crystal light emitters. In March 2000, he moved to St Andrews University, St. Andrews, U.K., where he is currently establishing a research group and setting up a semiconductor microfabrication laboratory.

Peter J. I. de Maagt (S'88–M'88–SM'02) was born in Pauluspolder, The Netherlands, in 1964. He received the M.Sc. and Ph.D. degrees from Eindhoven University of Technology, Eindhoven, The Netherlands, in 1988 and 1992, respectively, both in electrical engineering.

He is currently with the European Space Research and Technology Centre (ESTEC), European Space Agency, Noordwijk, The Netherlands. His research interests are in the area of millimeter and submillimeter-wave reflector and planar integrated antennas, quasioptics, photonic bandgap antennas, and millimeter- and sub-millimeter-wave components.

Dr. de Maagt was co-recipient of the H. A. Wheeler Award of the IEEE Antennas and Propagation Society for the best applications paper of the year 2001.